ISSN: 0975-8585

Research Journal of Pharmaceutical, Biological and Chemical Sciences

The Effect of Gelatin Types on the Synthesis of Magnetite Nanoparticles.

Lamyaa M. Abbas*.

Spectroscopic Department, Physics Division, National Research Center, El Behose st. Dokki , Cairo, Egypt.

ABSTRACT

Magnetic nanoparticles (Fe_3O_4) were synthesized in the presence of two different types of gelatin (A and B) by using coprecipitation method. The composition of the produced particles was determined by FTIR spectroscopy and thermogravimetric analysis (TGA). Both of transmission electron microscopy (TEM) and X-ray diffraction (XRD) were used for characterization of size and the crystallinity of the particles. The magnetic properties were studied by vibrating sample magnometers (VSM). TEM images indicated that Fe_3O_4 prepared in gelatin type A (GA) has particle sizes smaller than those prepared in gelatin type B (GB). TGA data indicated that the sample weight loss of gelatin of type (B) has been decreased by 44.234% while that of type (A) by 71.517%. VSM measurement showed that the magnetic nanoparticles prepared in the presence of either gelatin types have superparamagnetic behavior.

Keywords: gelatin A, gelatin B, iron oxide, nanoparticles, superparamagnetic, FTIR.

Corresponding author

ISSN: 0975-8585

INTRODUCTION

Gelatin is commonly used for pharmaceutical and medical applications because of its biodegradability and biocompatibility in physiological environments [1].

The natural sources of gelatin are animals. It is obtained by mainly acidic or alkaline, but also thermal or enzymatic degradation of the structural protein collagen. Collagen represents 30% of all vertebrate body protein. More than 90% of the extracellular protein in the tendon and bone and more than 50% protein in the skin consist of collagen [2].

According to the origin and pretreatment of the utilized collagen, two major types of gelatin are being commercially produced. Gelatin type A (**a**cid) is obtained from porcine skin with acidic pre-treatment prior to the extraction process. The second prevalent gelatin species, type B (**b**asic), is extracted from ossein and cut hide split from bovine origin. Thereby, an alkaline process, also known as "liming" is applied. During this extraction also the amide groups of asparagine and glutamine are targeted and hydrolyzed into carboxyl groups, thus converting many of the residues to aspartate and glutamate [3,4] Consequently, the electrostatic nature is affected. In contrast to collagen and gelatin type A having an isoelectric point (IEP) of pH 9.0, the higher number of carboxyl groups per molecule reduces the IEP to pH 5.0.

Magnetic nanoparticles such as magnetite have been widely used for in vivo biomedical applications including magnetic resonance imaging contrast enhancement [5-9], tissue specific release of therapeutic agents [10, 11], hyperthermia [12, 13] and magnetic field assisted radionuclide therapy [13].

All these applications require magnetic nanoparticles to be water soluble and biocompatible. Magnetic iron oxide nanoparticles are the primary choice because of their biocompatibility and chemical stability. Many synthesis methods have been explored for magnetic iron oxide nanoparticles. These include organic solvent heating method, polyol method, and co-precipitation method [15, 16, and 17]. The co-precipitation method is the most effective technique for preparing aqueous dispersions of iron oxide nanoparticles because the synthesis is conducted in water.

Some authors studied several biological molecules as surface coatings for nanoparticles to achieve biocompatibility such as dextran, agarose, cellulose, and albumin [18]. These molecules were used to control the particle size, to prevent the nanoparticles from aggregation, and to achieve biocompatibility.

Magnetic sponge-like hydrogels (ferrosponges) were produced by using an in-situ synthesis of magnetic nanoparticles in the presence of various concentrations of gelatin [19].

A magnetic hydrogels were fabricated by cross-linking of gelatin hydrogels and Fe_3O_4 nanoparticles (ca. 40–60 nm) through genipin as cross-linking agent for the development of a new magnetically induced drug delivery system [20].

This study aims to prepare magnetic nanoparticles in the presence of gelatin A and B types and find the effect of gelatin type on their synthesis and properties.

MATERIAL AND METHODS

All the chemicals used are analytical grad. gelatin type A and B (Aldrich), iron chloride hexahydrate (Riedel-deHaen), iron sulfate heptahydrate (fluka) and ammonium hydroxide 28 % (Edwek) were used in this experiment. Deionized water was deoxygenated by passing argon gas for 2 h before start.

In this experiment iron oxide nanoparticles were synthesized directly in the gelatin hydrogel by in-situ co-precipitation process with some modification of the method described elsewhere [19]. Briefly, the iron oxide nanoparticles in gelatin type B ($GBFe_3O_4$) was prepared through the following steps : 20 ml from 5% gelatin Type B solution were mixed with another equal amount of iron chloride hexahydrate and iron sulfate heptahydrate mixture with a molar ratio 2:1. The mixtures was stirred for 1 h at 40° C after which the mixture was left to cool at room temperature then incubate at 4° to be gel. Then, the gel block was immersed in 50 ml of ammonium solution the gel block turns to black due to the formation of iron oxide. The gel block

ISSN: 0975-8585

was washed several times till its pH reachs 7. The gel iron oxide block was re-melt by heating at 60° with stirring for 1h then the solution was sonicated at 25°.

The same steps were followed for the preparation of iron oxide in gelatin type A ($GAFe_3O_4$).

The samples were dried under vacuum for the measurements.

The Fourier transform infrared (FTIR) spectra of samples were recorded by Burker FTIR (VERTEX 70/80) instrument.

Thermal gravimetric analysis Shimadzu (Japan) N_2 Flow device was used to obtain TGA data of samples.

Transmittance electron microscope (TEM) image of samples were taken by JEOL JEM-2100 electron microscope. A drop of dried samples dispersed in ethyl alcohol was loaded on a grid and left to dry before measurement

X Pert panalatical X-ray diffraction (XRD) device with CuKα 40kV/30mA was used for recording the X- ray diffraction pattern of the sample.

Magnetic properties were measured through Vibrating Sample Magnometer (VSM) Lake shore 7410 USA.

RESULTS AND DISSCUTION

Fourier Transform Infrared Spectra (FTIR)

FTIR analysis was performed to confirm the formation of magnetic gelatin nano composite. Figure 1 shows the FTIR spectra of GA, GB, ($GBFe_3O_4$) and ($GAFe_3O_4$).

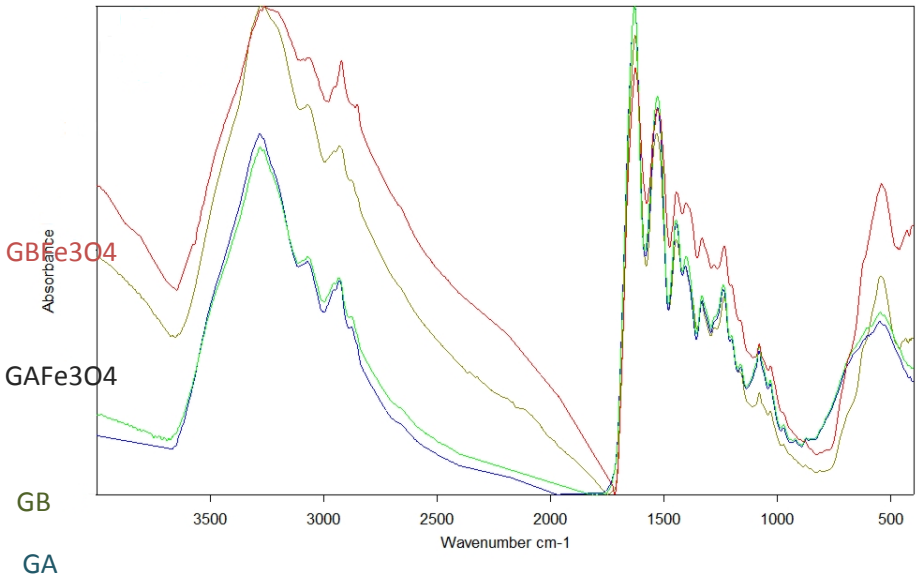

Figure 1: FTIR spectra of pure gelatin types (GA&GB) and gelatin with iron oxide nanoparticles ($GAFe_3O_4$& $GBFe_3O_4$).

Previously, it was reported that the characteristic absorption bands of the Fe-O bond of bulk Fe_3O_4 were at 570 -375 cm^{-1} [21]. However, when the size of Fe_3O_4 particles was reduced to nanoscale dimensions, the surface bond force constant increased due to the effect of finite size of nanoparticles, causing the breaking of a large number of bonds for surface atoms which resulted in the rearrangement of nonlocalized electrons on the particle surface. So that the absorption bands of IR spectra were shift to higher wavenumbers. So the blue-shift of absorption bands of the Fe_O bond of the Fe_3O_4 nanoparticles can be observed [22].

Researchers have investigated the interaction between a coating polymer and Fe_3O_4 particles [23- 27]. For instance, polymer interactions were studied in Fe/polypyrrole nanocomposites [24] and in Fe_3O_4 /polyaniline nanocomposites. They assumed interactions exist between the ione pair electrons of the N atom in the polypyrrole chain or in the polyaniline chain with the 3d orbital of the Fe atom to form a coordinate bond. Li et al. [25] reported that the interactive mechanism of oleic acid adsorption on the surface of Fe_3O_4 nanoparticles could be due to a hydrogen bonding or a coordination linkage. Zhang et al. [26] reported that poly (methacrylic acid) could adhere to Fe_3O_4 nanoparticles via coordination linkages between the carboxyl groups and iron.

For the spectra of GA, GB, GA Fe_3O_4 and GB Fe_3O_4 Fig.(1), it is noticed that all the spectra have absorption bands at 3280 cm^{-1}, that represent N-H str. of amide A, and a band at 3072 cm^{-1} which belong to C-H stretching vibration [28,29]. A band observed at 1629 cm^{-1} for GA and GB is shifted to 1627 and 1626 cm^{-1} for GA Fe_3O_4 and GB Fe_3O_4 spectra respectively. This band is assigned to C=O stretching vibration of amide I. Another band is found at 1529 and 1528 cm^{-1} for the spectra of GA and GB respectively is shifted to 1533 and 1531 cm^{-1} in case of GA Fe_3O_4 and GB Fe_3O_4 spectra respectively. A small peak is present at 549 and 530 cm^{-1} for GA and GB spectra respectively, while this peak became strong and narrow for GA Fe_3O_4 and GB Fe_3O_4 spectra and is observed at 544 and 541 for them respectively. In addition, a new small peak is observed at 428 and 430 cm^{-1} for GA Fe_3O_4 and GB Fe_3O_4 spectra respectively. Two absorption bands at about 540 and 430 cm^{-1} are defined as Fe-O bond [22].

The results indicated that the a shift in the position of the band of amide I and II in GA Fe_3O_4 and GB Fe_3O_4 spectra may be due to the interaction of Fe_3O_4 with gelatin through the amid groups. Hence the changes in absorption of the band at about 541 and the appearance of a small band at about 430 cm^{-1} in the spectra of GA Fe_3O_4 and GB Fe_3O_4 confirmed the formation of Fe_3O_4 particle in nano size.

Transmittance Electron Mmicroscope (TEM)

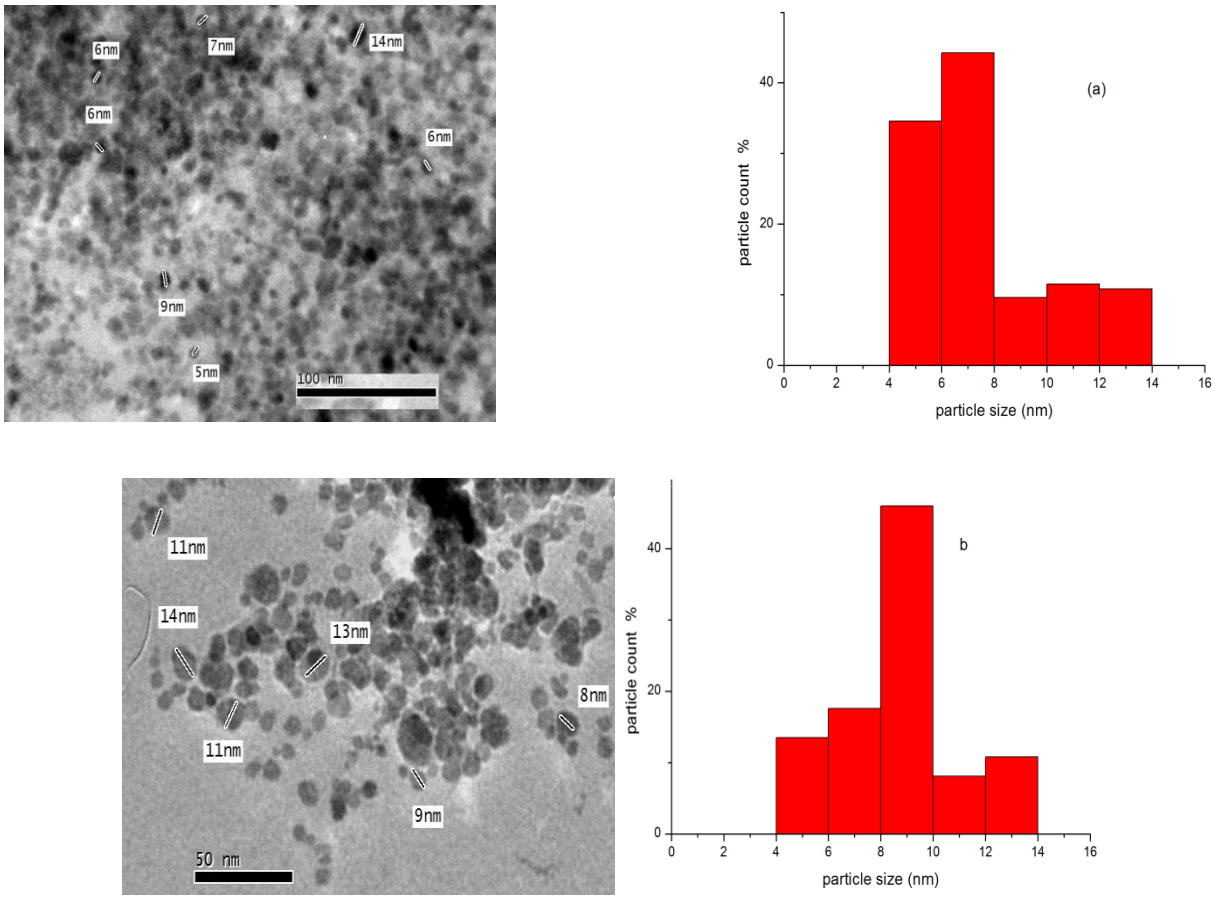

Figure 2: TEM image and particles distribution of Fe_3O_4 with gelatin types A (a) and B (b).

ISSN: 0975-8585

TEM images of GA Fe_3O_4 and GB Fe_3O_4 and their particle distribution are given in Fig. (2). It is noticed that the prevailing particle sizes of Fe_3O_4 prepared in GA are observed between 4-8 nm and reach its maximum in the range 6-8 nm while those prepared in GB are in range 8-10 nm . This result indicated that Fe_3O_4 prepared in GA has particle sizes smaller than those prepared in GB.

Thermal Gravimetrical Analysis (TGA)

Fig. (3) illustrates the TGA curve for GA Fe_3O_4 and GB Fe_3O_4. From a previous work it was found that the TGA curve of pure Fe_3O_4 nanoparticles had no significant weight loss [30]. Whereas, it is clear from Fig. (3) that there are distinct weight losses in the TGA curves of GA Fe_3O_4 and GB Fe_3O_4 nanoparticles. The initial weight loss is 11 % for GA Fe_3O_4 that is observed at 31.4°C up to 119.24 °C whereas that for GB Fe_3O_4 nanoparticles is 12.8% which starts at 30.25°C up to 257.8 °C. This weight loss is due to the moisture content and dehydration reaction of –OH groups of both samples. The second weight losses are 60 % (at 119.2 up to 501.8 °C) and 31.2 % (at 257 up to 431°C) for GA Fe_3O_4 and GB Fe_3O_4 nanoparticles respectively. This weight loss is referred to the decomposition of gelatin of the samples releasing CO_2 gas. It is noticed that the rate of weight loss for GB Fe_3O_4 nanoparticles sample is slower than that of GA Fe_3O_4. This indicated the more thermo stability of GB Fe_3O_4 nanoparticles sample compared to that of GA Fe_3O_4. This may be due to the fact that GB molecules has more coordination bonds with iron than those in case of GA. As derived from their TGA curves the percentage of Fe_3O_4 content is 29% and 56% GA Fe_3O_4 and GB Fe_3O_4 samples respectively.

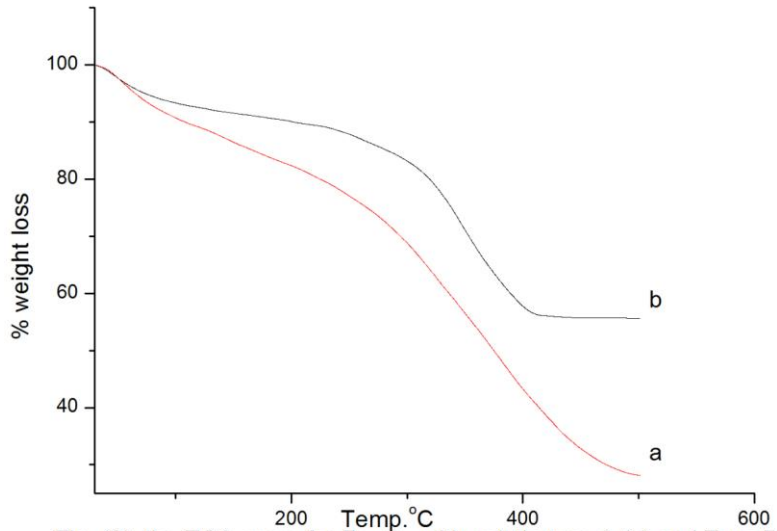

Fig. (3) the TGA curve for Fe_3O_4 with gelatin type A (a) and Type B (b).

X ray diffraction (XRD)

The XRD patterns of GA Fe_3O_4 and GB Fe_3O_4 nanoparticles are shown in Fig. (4). From this fig, It observed that The XRD patterns for both samples have the characteristic diffraction peaks at 2Θ = 30.14º, 35.43 º, 43.11º, 53.55º, 57.10º and 62.7º which are matching well with that of standard Fe_3O_4 cubic crystalline (card no. 01-079-0418). This reveals that Fe_3O_4 particles synthesized in either types of gelatin are of crystalline structure.

Magnetic Properties

The hysteresis of GA Fe_3O_4 and GB Fe_3O_4 is given in Fig. (5). It can be seen from this fig. that, the saturation magnetization for GA Fe_3O_4 and GB Fe_3O_4 particles are 6.0927 emu/g and 3.3693 emu/g respectively, which are lower than that of bulk magnetite (98 emu/g) [58]. This result shows that Fe_3O_4 synthesis in GB has superparamagnetic behavior higher than those prepared in GA. The lowering in saturation magnetization can be attributed to the reduction of the particles sizes and gelatin coated on the surface of Fe_3O_4 nanoparticles which acts as nonmagnetic layer. In addition, the particles have a very low coercivity which is 0.16350 G for GA Fe_3O_4 and 2.4620 G for GB Fe_3O_4. Also both samples have a very low retentivity which are 1.0486E-6 emu/g and 6.9590E-3 emu/g for GA Fe_3O_4 and GB Fe_3O_4 respectively. These results

ISSN: 0975-8585

indicate that the prepared Fe_3O_4 particles in both gelatin types are in nano sizes and have superparamagnetic behavior.

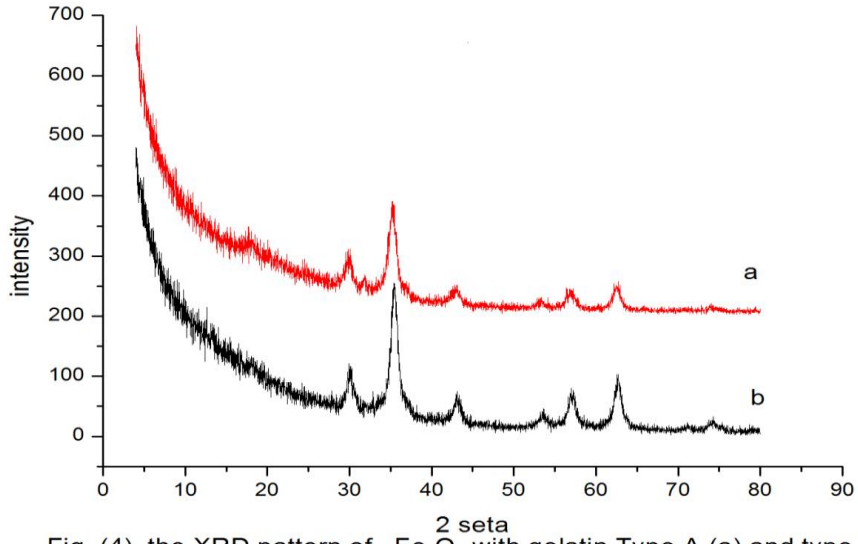

Fig. (4) the XRD pattern of Fe_3O_4 with gelatin Type A (a) and type B (b).

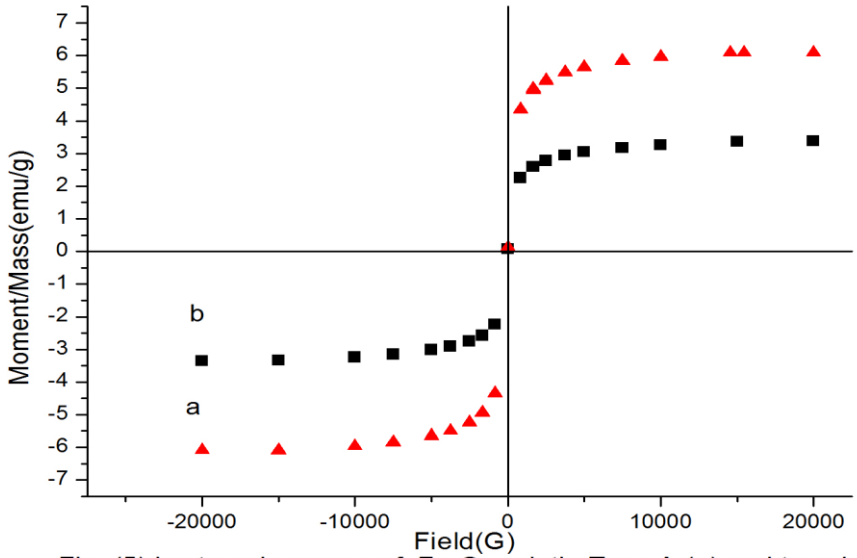

Fig. (5) hysteresis curves of Fe_3O_4 gelatin Type A (a) and type b (b).

CONCLUSION

From this study it can be concluded that the Fe_3O_4 particles prepared in GA has particle sizes smaller than those prepared in GB. GB molecules have more coordination bonds with iron than those in case of GA. Fe_3O_4 particles synthesized in either type of gelatin are in nano sizes, and have crystalline structure and superparamagnetic behavior.

ACKNOWLEDGMENT

I would like to express my sincere gratitude to Professor Dr. Ahmad Abd el Rahman Fakhry for his effort and cooperation in reviewing this manuscript.

REFERENCES

[1] Yao C H, Liu B S, Hsu S H , Chen Y S, Tsai C C. J Biomed Mater Res 2004; 69A: 709– 717.
[2] Friess, W. Eur J Pharma and Biopharma 1998; 45(2): 113-136.

[3] Tabata Y, Ikada Y Adv Drug Delivery Rev1998; 31(3): 287-301.
[4] Young S, Wong M, Tabata Y, Mikos A G. J of Controlled Release 2005; 109: 256 -274.
[5] Weissleder R, Bogdanov A, Neuwelt EA, Papisov M. Adv Drug Delivery Rev 1995; 16: 321–34.
[6] Reimer P, Weissleder R. Radiologe 1996; 36:153– 163.
[7] Chouly C, Pouliquen D, Lucet I, Jeune JJ, Jallet P. J Microencapsulation 1996; 13: 245–255.
[8] Okon E, Pouliquen D, Okon P, Kovaleva ZV, Stepanova TP, Lavit SG, Kudryavtsev BN, Jallet P. Lab Invest 1994; 71: 895–903.
[9] Jung CW, Jacobs P. Magn Reson Imaging 1995; 13: 661–674.
[10] Gupta PK, Hung CT. Life Sci 1989; 44: 175–186.
[11] Lubbe AS, Bergemann C, Huhnt W, Fricke T, Riess H, Brock JW, Huhn D. Cancer Res 1996; 56: 4694–4701.
[12] Chan D C F, Kirpotin D, Bunn PA. J Magn Magn Mater 1993; 122: 374–378.
[13] Jordan A, Wust P, Scholz R H, Afeli U, Sch W utt, Teller J, Zborowski M. editors. Scientific and clinical applications of magnetic carriers. New York: Plenum Press, 1997. p. 569.
[14] uttner C Gr, Teller J, Sch W Utt, H. In, U Afeli, Teller J, Zborowski M, editors. Scientific and clinical applications of magnetic carriers. New York: Plenum Press, 1997. p. 53.
[15] Ge JP, Hu YX, Biasini M, Dong CL, Guo JH, Beyermann WP & Yin YD. Chem Eur J 2007; 13(25):7153-7161.
[16] Hyeon T. Chemical Commun 2002; 8:927- 934.
[17] Wenguang Y, Tonglai Z, Jianguo Z, Jinyu G & Ruifeng W. Prog Chem 2007, 19(6):884-892.
[18] Chatterjee J, Haik Y, Chen C J. J Magn Magn Mater 2001; 225: 21-29.
[19] Shang-Hsiu H, Ting-Yu L, Dean-Mo L, San-Yuan C. J Controlled Release 2007; 121: 181–189.
[20] Ting-Yu L, Shang- Hsiu H, Kun-Ho L, Dean-Mo L, San-Yuan C. J Magn Magn Mater 2006; 304: e397–e399.
[21] Waldron R D. Phys Rev 1955; 99: 1727-1735.
[22] Ming M, Yu Z, Wei Y, Hao-ying S, Hai-qian Z, Ning G. Colloids and Surfaces A: Physicochem. Eng. Aspects 2003; 212: 219-226.
[23] Deng J G, Peng Y X, He C L; Long X P; Li P, Chan A S C. Polym Int 2003; 52 (7): 1182–1187.
[24] Deng J, Ding X, Zhang W, Peng Y, Wang J, Long X, Li P, Chan A S C. Polymer 2002; 43: 2179–2184.
[25] Li P, Yu B, Wei X. J Appl Polym Sci. 2004; 93: 894–900.
[26] Zhang H, Wang R, Zhang G, Yang B. J Appl Polym Sci 2003; 429: 167–173.
[27] Ma H, Qia X, Maitani Y, Nagai T. Int J Pharm 2007; 333(1):177–186.
[28] Hector L C, Henry H M. Biochimic et Biophyic Acta 1984; 779: 381-401.
[29] Manule A C, António B, Mário B, Douglas N R, Ivonne D. Carbohyd Polym 1998; 37:241-248.
[30] Lamyaa M A. Res J Pharm Biol Chem Sci 2015; 6(6) in press.
[31] Cullity B. D. Introduction to Magnetism and Magnetic Materials; Addison-Wesley: MA, 1972.